

Slow modulation of the contraction patterns in *Physarum polycephalum*

Raphael Saiseau,^{1,2,*} Valentin Busson,¹ and Marc Durand^{1,†}

¹Laboratoire MSC, Université de Paris, CNRS, UMR 7057, Matière et Systèmes Complexes (MSC), F-75006 Paris, France.

²Department of Physics, University of Konstanz, Konstanz 78457, Germany

Physarum polycephalum, a biological transport network, has emerged as a model for the study of self-organisation and coordination at large spatial scales. This self-organisation is largely due to cytoplasmic fluid flows driven by propagating contractile waves that are delocalised over the entire organism. Furthermore, complex modulation of these contractile waves on long time scales has also been observed, but is scarcely studied. In this study, we comprehensively characterise this long-time scale modulation by confining the organism within ring geometries. Our findings reveal a clear correlation between contractile wave direction, amplitude modulation, and the moving mean vein diameter. We observe simultaneous spatio-temporal travelling and standing wave patterns that bear a resemblance to the ring oscillating fundamental modes. Furthermore, we ascertain that the time periods of these modes scale with the system size and correspond to multiples of the statistically observed intrinsic modulation time scale. This suggests the presence of a common mechanism. These findings serve to reinforce the hypothesis that the flows patterns modulation is the result of the transport of a chemical agent responsible for modifying the local rigidity of the membrane, which would act as a signaling mechanism for the organism.

Flows over remarkably long distances are crucial to the functioning of many organisms, across all kingdoms of life. These coordinated flows are required for migration, development, and the dissemination of resources and signals. Nevertheless, the mechanisms that facilitate such coordination remain to be fully elucidated, with the relative importance of chemical and mechanical factors/feedback remaining to be fully ascertained.

For instance, an ubiquitous mechanism to generate flows, particularly prominent in animals and amoebas, is actomyosin cortex-driven mechanical deformations that pump the fluid enclosed by the cortex. Chemicals as calcium or cAMP are known to play a role in the regulation of the contractile activity of the actomyosin cortex. Advection of these chemicals along with the flow then certainly take an important place in the coordination of the contractions. However, mechanical stress generated by the incompressible flow must also couple contractions to satisfy the volume conservation. Moreover, subtle mechano-chemical couplings can also take place, such as the action of stress on mechano-sensitive channels that in turn affect the concentration of chemicals. It is also known that the action of external forces alter the contractions of the cortex, and induce a reorganisation of the actomyosin fibers.

A particularly well-suited organism for studying such large-scale cytoplasmic flows is *Physarum polycephalum*, a multinucleated unicellular organism that takes the form of a centimetre-sized network. A striking feature of this organism is the presence of regularly organised contractile oscillations of its actomyosin cortex, which drive large-scale cytoplasmic flows throughout its network. These oscillations manifest as well-defined travel-

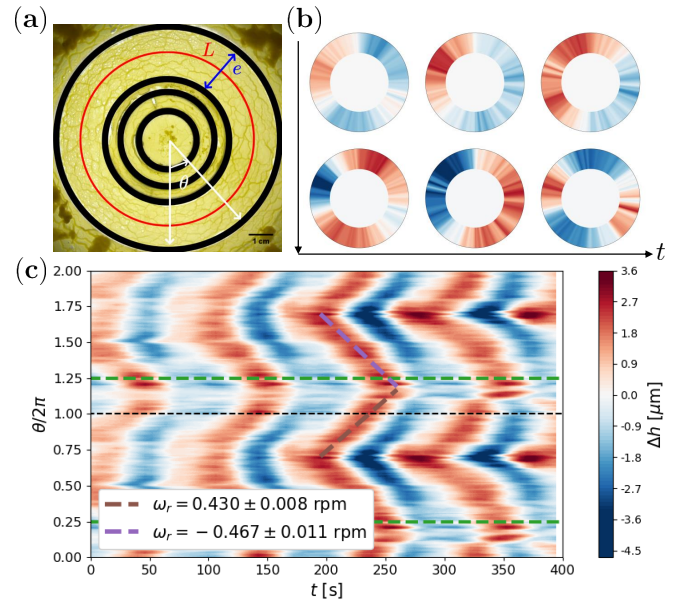


Figure 1. (a) Raw image of an initially homogeneous specimen cropped with three concentric annular punches. The ring perimeter L and width e are indicated. (b) Representation of height variation along the ring at successive times showing counter-propagative waves. (c) Corresponding space-time plot.

ing waves, with a time period of 100 s time period and a wavelength equal to its body size [1], which corresponds to optimal nutrient transport throughout the organism [2].

These contractile activity oscillations have been the subject of some experimental characterisations showing the travelling nature of this oscillation [3], its relation to system geometry and size [4], its scale-adapting property and spatial pattern [1] and its relation to migration

* raphael.saiseau@uni-konstanz.de

† marc.durand@univ-paris-diderot.fr

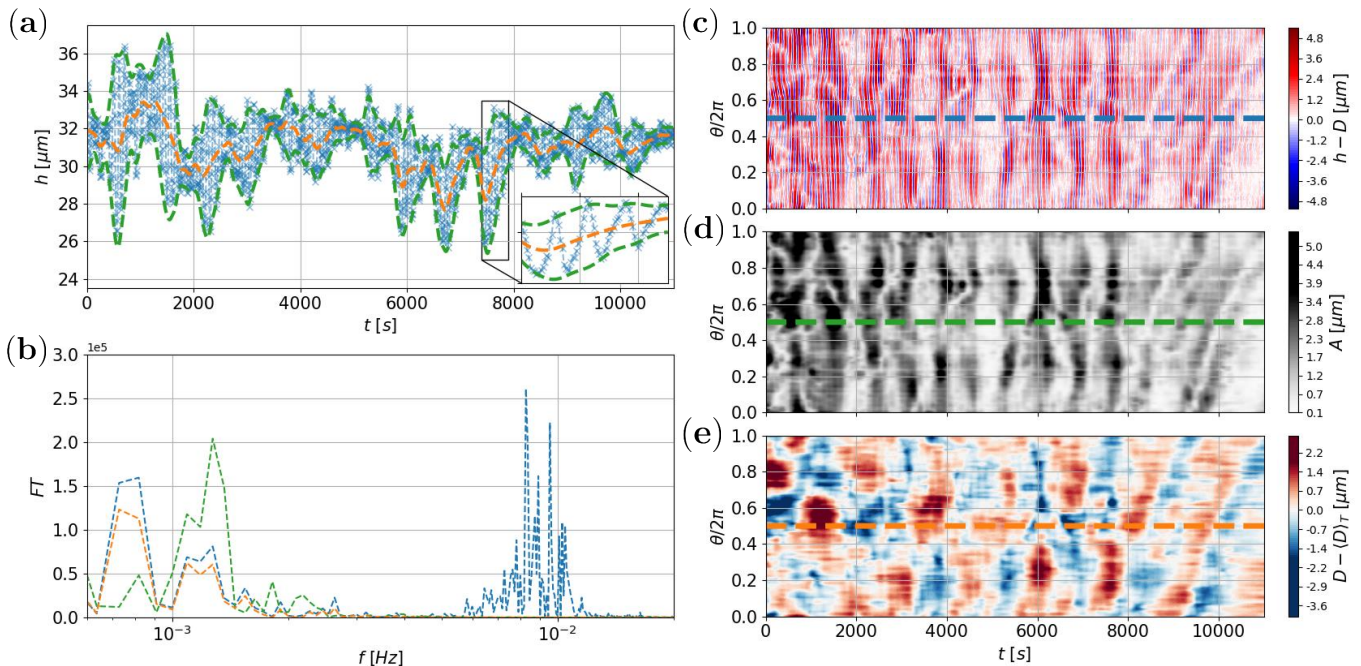


Figure 2. (a) Height variations oscillating signal for ring position $\theta = \pi$ over time. Amplitude and drift defined equation (1) are also shown. (b) Corresponding Fourier spectra of the height variations, amplitude and drift shown in (a). (c) Kymograph showing the short time height oscillations around its slow drift value $h(\theta, t) - D(\theta, t)$, (d) its corresponding modulation signal $A(\theta, t)$ and (e) its drift D .

[5] and to network dynamics [6]. On the contrary, amplitude modulation [5], mean vein diameter growth [7] and wave direction variations [1] have been observed on typical timescales of 15 – 40 min, but have never been the focus of a specific study. Interestingly, these long timescale dynamics show a surprising ubiquity, and have also been reported in different contexts: from ambiguous spontaneous variations [3, 4, 8] to well-characterised responses to stimuli or harm [7, 9–11]. This suggests a common mechanism underpinning all these diverse observations of fundamental importance to the organism.

MATERIAL AND METHODS

Here we propose to characterise in more detail these long-term contractions on a controlled simple one-dimensional geometry. This is achieved by confining an initially homogeneous *Physarum* plasmodium in concentric cylindrical walls to form plasmodial rings with typical aspect ratios ranging from 11 to 41, then defined only by the main axis radius R . These ring confined plasmodia are then observed using a transmission microscopy setup with the blue channel of a Basler colour CMOS camera to obtain the thickness dynamics $h(t, \theta)$, where θ is the angular position on the ring. In this ring geometry, the spatial patterns of contraction oscillations have already been characterised, showing a dominant counterpropagative wave pattern (see Figure 1). To obtain longer time scales, we decompose the plasmodium thickness h as fol-

lows:

$$h(t, \theta) - \langle h \rangle_T = D(t, \theta) + A(t, \theta) \cos[\phi(t, \theta)] \quad (1)$$

where ϕ is the phase of the contraction oscillations, A is the oscillations amplitude and D a slow drift. $\langle h \rangle_T$ corresponds to the moving average on a 3000 s time window to smear out the dynamics of network reorganisation [6], which is not considered here.

Figure 2 shows an example of the spatial patterns and time evolution of h , A and D . Looking at their dynamics, their corresponding Fourier transform shows a separation of time scales where A and D have a slower dynamics than ϕ with a 10^3 s time scale. Their corresponding spatial patterns also show distinctive features with observable travelling and standing wave patterns for both A and D . This restores the broken symmetry of ϕ counterpropagative waves pattern shown in Figure 1. It should be noted that we have chosen to show a transition between two successive patterns, which we will call the rotating and standing modes, in order to demonstrate its suddenness.

RESULTS

In this section, the observed amplitude and drift patterns presented in Figure 2 are discussed. In comparison to the height oscillations associated with shuttle flows, the amplitude and drift exhibit spatial patterns that are

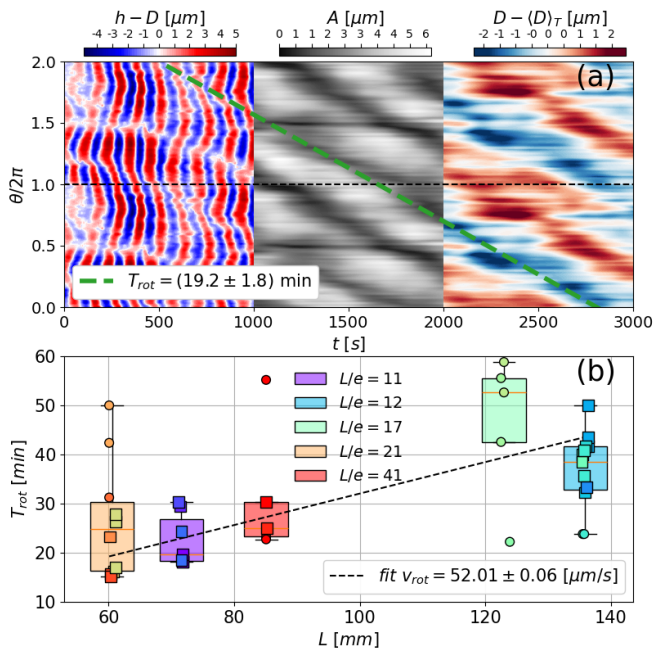


Figure 3. (a) Example of rotating pattern seen in a kymograph of height oscillation around drift value $h(\theta, t) - D(\theta, t)$, its amplitude modulation $A(\theta, t)$ and the drift variations $D(\theta, t) - \langle D(\theta, t) \rangle_T$ with $\langle D(\theta, t) \rangle_T$ a running mean value with a time window $T = 3000$ s. A linear fit of the isophase in amplitude modulation A gives an example of revolution period of amplitude signal T_{rot} . (b) Rotation period of amplitude modulation T_{rot} over ring perimeter L . Square markers correspond to rotating patterns while round markers correspond to counter-rotating patterns or rotating waves harmonics. Colors correspond to the aspect ratio of the corresponding ring. A linear fit gives a transport speed of amplitude signal along the ring v_{rot} independent of Physarum ring size.

less frequently coordinated at the system scale. Higher-order spatial harmonics and even patterns superimposed on independent dynamics can be observed. In the experimental sets under consideration, structured signals at the system size are observed more frequently for rings with large radii and widths, which may be associated with a more reticulated network. This latter point is supported by the total absence of rotating patterns in amplitude and drift patterns for locally dying or cut rings.

We focus now on standing or rotating waves patterns in a broad sense, incorporating counter-rotating patterns and rotating waves harmonics. These patterns account for 38% of the total time of the experiments. Rotating patterns predominate, accounting for 88% of the observed patterns, while standing patterns are observed only as transitions, particularly between two rotating modes of opposite direction. Among the rotating patterns, the fundamental mode of a single rotating wave is observed 60% of the time, thus establishing itself as the most dominant pattern.

It is noteworthy that these rotating patterns exhibit remarkable stability, with a mean duration of 1.00×10^4 s

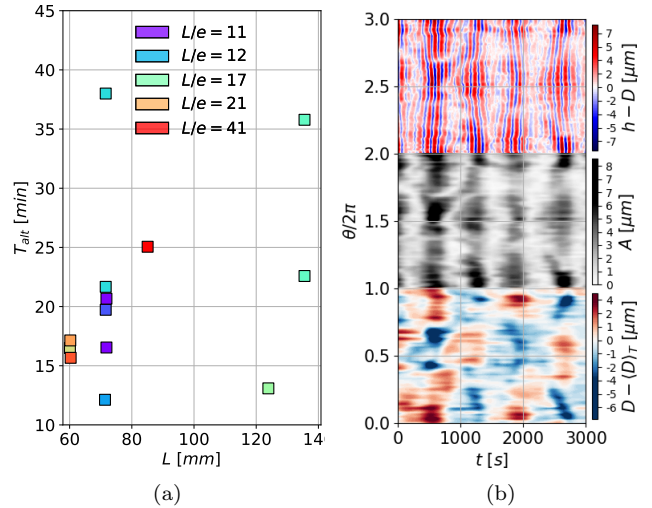


Figure 4. (a) Alternative time period T_{alt} over ring perimeter L corresponding to the alternative pattern shown in (b) the kymograph of height oscillations $h(\theta, t) - D(\theta, t)$, modulation amplitude $A(\theta, t)$ and drift $D(\theta, t)$.

and a standard deviation of 0.51×10^4 s, extending over 2.0×10^4 s. Furthermore, these patterns can show sudden change in the rotation direction. This time scale is reminiscent of the network growth and reorganization time scale observed for the same experiments, suggesting that they are indeed stable modes in the absence of network architectural change. In comparison, standing wave patterns are typically characterised by significantly shorter durations, with a mean value of 0.51×10^4 s and a standard deviation of 0.21×10^4 s. As illustrated in Fig.3(b), the fitted revolution period of rotating patterns is proportional to the perimeter of the ring L , measured at its main axis. This results in a constant rotation speed, v_{rot} of $52 \mu\text{m/s}$, which is compatible with the amplitude modulation velocity measured in [12]. In comparison to the rotating pattern, the scaling with the ring perimeter is more challenging to ascertain for standing waves patterns, yet it demonstrates a time period that is generally around 1000 s.

In this part, a comparison is made between the observed modulation patterns and the primary height oscillation. As was already reported for the drifted counter-propagative waves in [1], the observed patterns demonstrate a clear correlation with the direction of phase traveling waves. The height oscillations show a source and sink points at opposing locations, establishing a polarity axis that undergoes rotation or alternation for rotating or standing waves, respectively. This polarity axis is also superimposed with the observed asymmetry between contraction and dilatation and the drift gradient main axis, as seen for the drift rotating mode (Fig.3(a)) and for the standing wave (Fig.4(b)).

Such clear patterns are observed preferentially on networks showing clearly observable and large central veins

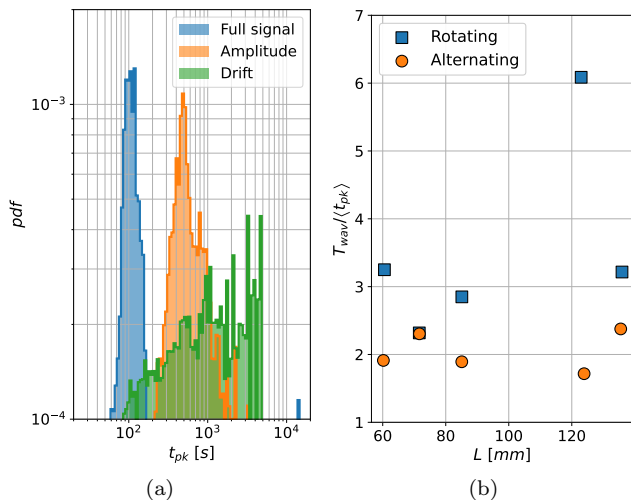


Figure 5. (a) Weighted density histograms of the maxima peak locations in the Fourier spectra of respectively the full height oscillation h , its corresponding amplitude modulation A and drift D for all ring experiments with a perimeter $L = 60$ mm. (b) Rotating and alternative patterns time periods compared to the statistical most probable dominant mode in amplitude Modulation Fourier spectrum.

(see Fig.6(a) and (b) in Supplementary material).

Statistical approach of modulation time scale

In order to generalise the contractile activity modulation analysis made on the most representative cases shown in Figures 3 and 4, the Fourier analysis on the modulation signal shown in Figure 2 is systematised. For a given ring experiment, the Fourier spectra dominant frequency is derived for each angular position, and is weighted by its corresponding power spectrum maximum. A distribution is computed for each ring experiment. The resulting mean weighted dominant frequency distribution obtained for all experiments with a ring perimeter $L = 60$ mm is shown in Figure 5(a). At this stage, the amplitude modulation signal is preferred to the drift signal in order to achieve a significant amount of signal repetition during the 10^4 s network reorganization time frame.

As demonstrated in the example shown in Figure 2, for $L = 60$ mm a clear and distinctive amplitude time scale is observed at $T = 485$ s. This peak value is compared in Figure 5(b) to the rotational and alternative patterns periods. It is observed that, while the alternative pattern time period is equal to the drift time scale, for the rotational pattern revolution time, it is generally given by 1.5 times the drift time scale. Since spatially stable patterns are a multiple of the modulation signal spontaneous intrinsic time scale, this suggests that amplitude modulation oscillations are spontaneous and that their synchronization generates these modes. This synchro-

nization mechanism appears to be well correlated to the network growth and reorganization, which was analysed in detail in [6].

DISCUSSION

The present study reports the long-time scale evolution of the contractile activity of *Physarum polycephalum* trapped in a ring geometry. This geometry has been chosen as a model system to avoid polarity issues and to explore its contractile modes in a simplified geometry, facilitating signal treatment by removing the network complex and evolving architecture from the analysis. The exploration of contractile oscillations is conducted on time scales shorter than the network reorganization timescale (10^4 s [6]). The height variations are decomposed using a drift value, an amplitude modulation, and a phase, all depending on time and on the angular position on the ring.

Short time scales dynamics are obtained from the phase, and a typical time scale of 10^2 s is observed along with a counterpropagative waves pattern that has distinctive source and sink points, thereby breaking the imposed symmetry of the system [1]. Longer time scales are then obtained from the drift and amplitude modulation evolution, and show clear intrinsic time scale and spatial patterns of the order 10^3 s in the explored parameter range. Interestingly, a clear relationship is observed between amplitude modulation and drift. Specifically, amplitude modulation defined positively is perfectly given by the absolute value of the drift.

The spatio-temporal patterns of the drift are then reported, and it is observed that the dominant pattern is a single rotating mode, thereby restoring the ring symmetry of the system. While more complex rotating patterns can also be found, these show a time period of revolution compatible with a constant wave velocity. Standing wave patterns are also observed, despite more often as transient regimes. Both modes seem to be related to well-developed networks following the ring symmetry. The existence of a relationship between these two modes and the spontaneous signal modulation oscillations is indicated by the fact that their time periods are multiple of the intrinsic modulation oscillations' temporal scale, thereby suggesting a self-synchronization mechanism.

Finally, it is to be noted that this work opens the way to an interesting outcome: the capacity to retrieve the rigidity mapping of the network and the contractile activity throughout the system by monitoring the long-term evolution of vein sizes. This development promises to provide novel analytical tools that are more cost-effective to facilitate the reconstruction of the complete contractile activity of the organism. More fundamentally, this suggests that the main mechanism to explain the contractile activity distribution and coordination lies in a

long time intrinsic mechanism acting on preferentially as a signal modulation. Understanding this yet unexplored mechanism would therefore be of utmost importance to finally obtaining the keys to unlocking the door behind its smart behavior.

ACKNOWLEDGMENTS

We acknowledge financial support from French National Research Agency Grants ANR-17-CE02-0019-01-SMARTCELL and CNRS MITI ‘Mission pour les initiatives transverses et interdisciplinaires’ (reference: BioRes).

-
- [1] V. Busson, R. Saiseau, and M. Durand, Phase patterns in slime mould confined in a ring geometry, *PNAS* **16**, 802 (2020).
 - [2] K. Alim, G. Amselem, F. Peaudecerf, M. P. Brenner, and A. Pringle, Random network peristalsis in physarum polycephalum organizes fluid flows across an individual, *Proceedings of the National Academy of Sciences* **110**, 13306 (2013).
 - [3] P. Fleig, M. Kramar, M. Wilczek, and K. Alim, Emergence of behaviour in a self-organized living matter network, *Elife* **11**, e62863 (2022).
 - [4] S. Kuroda, S. Takagi, T. Nakagaki, and T. Ueda, Allometry in physarum plasmodium during free locomotion: size versus shape, speed and rhythm, *Journal of experimental biology* **218**, 3729 (2015).
 - [5] C. Oettmeier and H.-G. Döbereiner, A lumped parameter model of endoplasm flow in physarum polycephalum explains migration and polarization-induced asymmetry during the onset of locomotion, *PloS one* **14**, e0215622 (2019).
 - [6] R. Saiseau, V. Busson, L. Xénard, and M. Durand, Network emergence and reorganization in confined slime moulds, *Journal of Physics D: Applied Physics* **57**, 145401 (2024).
 - [7] M. Kramar and K. Alim, Encoding memory in tube diameter hierarchy of living flow network, *Proceedings of the National Academy of Sciences* **118** (2021).
 - [8] R. Mayne, J. Jones, E. Gale, and A. Adamatzky, On coupled oscillator dynamics and incident behaviour patterns in slime mould physarum polycephalum: emergence of wave packets, global streaming clock frequencies and anticipation of periodic stimuli, *International Journal of Parallel, Emergent and Distributed Systems* **32**, 95 (2017).
 - [9] T. Nakagaki, H. Yamada, and T. Ueda, Interaction between cell shape and contraction pattern in the physarum plasmodium, *Biophysical chemistry* **84**, 195 (2000).
 - [10] Y. Yoshimoto, F. Matsumura, and N. Kamiya, Simultaneous oscillations of ca²⁺ efflux and tension generation in the permealized plasmodial strand of physarum, *Cell motility* **1**, 433 (1981).
 - [11] F. K. Bäuerle, M. Kramar, and K. Alim, Spatial mapping reveals multi-step pattern of wound healing in physarum polycephalum, *Journal of Physics D: Applied Physics* **50**, 434005 (2017).
 - [12] K. Alim, N. Andrew, A. Pringle, and M. P. Brenner, Mechanism of signal propagation in physarum polycephalum, *Proceedings of the National Academy of Sciences* **114**, 5136 (2017).

Appendix A: Physarum network examples

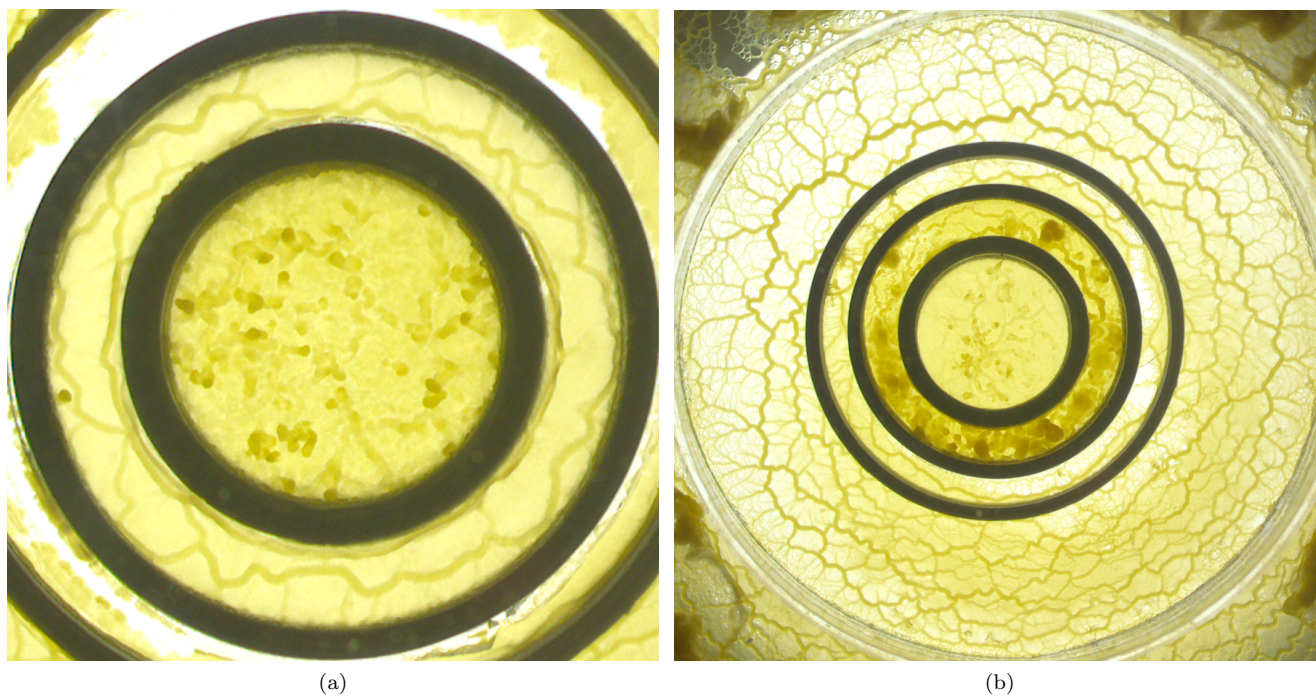


Figure 6. Examples of Physarum network corresponding (a) to the rotating pattern shown in Fig.3 and (b) to the alternative pattern shown in Figure 4.